CMS Physics Analysis Summary

Contact: cms-pag-conveners-heavyions@cern.ch 2023/07/31

Net-charge fluctuations in PbPb collisions at $\sqrt{s_{\mathrm{NN}}} = 5.02\,\mathrm{TeV}$

The CMS Collaboration

Abstract

Net-charge fluctuation measurements for lead-lead (PbPb) and proton-proton (pp) collisions at $\sqrt{s_{\mathrm{NN}}}$ = 5.02 TeV are presented. The PbPb and pp data were obtained with the CMS detector at the CERN LHC and correspond to integrated luminosities of 0.607 and 252 nb^{-1}, respectively. A measure of the relative strength of the correlated pairs is determined for a wide range of relative pseudorapidity (with $\Delta\eta < 4.8$) and in different centrality intervals using reconstructed tracks with transverse momenta in the range 0.5–3.0 GeV. An excess of opposite sign pairs is observed that increases with the charged-particle multiplicity.

1 Introduction

Ultrarelativistic heavy ion collisions can be used to study the properties of the hot and dense state of matter, known as quark-gluon plasma (QGP), formed in these collisions [1–9]. A number of observables have been used to explore the properties of the QGP and to establish the associated phase transition diagram in quantum chromodynamics (QCD). The measurement of event-by-event fluctuations of the conserved quantities, such as the net-charge, net-baryon, or net-strangeness numbers [10, 11], are frequently used as tools for characterizing the thermodynamic properties of the transition from the QGP to the hadron resonance gas (HRG) phase. The net-charge fluctuations are proportional to the square of the charge associated with individual charge carriers in the system [12–14]. In the QGP phase the quarks carry fractional electric charge ($\pm\frac{2}{3}e, \pm\frac{1}{3}e$), whereas in the HRG phase the charge carriers all have unit charge ($\pm 1e$). Therefore, net-charge fluctuations in the QGP phase are expected to be smaller than those in the HRG phase [12, 13, 15–17]. Hence, charge fluctuations measurements can probe the QGP. It is also argued that, if the initial QGP phase is primarily dominated by gluons, the fluctuations per entropy may be lowered further as gluon hadronization increases the entropy [11–13]. The reduction in fluctuations appears as a further means of identifying the formation of QGP in high-energy heavy ion collisions.

Net-charge fluctuations can also be affected by volume fluctuations. A quantity that is sensitive to the net-charge fluctuations while cancelling out some of the effects of volume fluctuations is the variance of the ratio of the numbers of positive (N_+) and negative (N_-) charges in the system, δR, with $R = \frac{N_+}{N_-}$. The net charge is given by $Q = N_+ - N_-$, and has variance δQ. The dynamical net-charge fluctuations per unit entropy is given by the so-called "D" parameter, which can be related to the variances of R and Q, with

$$D = \langle N_{\rm ch}\rangle \langle \delta R^2\rangle = 4\frac{\langle \delta Q^2\rangle}{\langle N_{\rm ch}\rangle}, \tag{1}$$

where $N_{\rm ch} = N_+ + N_-$ and $\langle ...\rangle$ denotes an average over an event ensemble. These quantities are typically measured in certain transverse momentum ($p_{\rm T}$) and pseudorapidity (η) intervals [17].

The value of D is estimated considering several theoretical predictions including lattice QCD calculations. According to theoretical calculations, the value of D for the HRG phase is roughly equal to 4 [12, 13, 16, 17]. The correlations between $\rm N_+$ and $\rm N_-$ can be reduced by neutral resonances. The existence of resonances is anticipated to decrease the D value to 3 in the HRG phase [12, 13, 16, 17]. The D value is 1–1.5 for a QGP phase, where the uncertainty arises from relating the entropy to the number of charged particles $\langle N_{\rm ch}\rangle$ [12, 13, 16, 17]. Various effects from hadronization, e.g., resonances, diffusion, and thermalization might also complicate the measurement and interpretation of net-charge fluctuations. However, there is a significant difference of at least 2 to 3 units in the D between the HRG and QGP phases, which can be explored experimentally.

An observable that can be related to the net-charge fluctuations, $\nu_{(+-,\rm dyn)}$, is expressed in terms of the relative correlation of particle pairs, with

$$\nu_{(+-,\rm dyn)} = \frac{\langle N_+(N_+-1)\rangle}{\langle N_+\rangle^2} + \frac{\langle N_-(N_--1)\rangle}{\langle N_-\rangle^2} - 2\frac{\langle N_+N_-\rangle}{\langle N_-\rangle\langle N_+\rangle}. \tag{2}$$

The measured ratios are independent of detector efficiency and acceptance as these effects are

similar for the numerator and denominator of each term and, consequently, largely cancel in the ratios [10]. Negative (positive) values of $\nu_{(+-,\mathrm{dyn})}$ indicate the dominance of correlations due to opposite-sign (same-sign) pairs. The entropy produced in a medium is proportional to the number of charged particles. The relationship between $\nu_{(+-,\mathrm{dyn})}$ and D [17] is given by

$$\langle N_{\mathrm{ch}} \rangle \nu_{(+-,\mathrm{dyn})} = D - 4. \tag{3}$$

The average value of $\mathrm{N_{ch}}$, calculated in different centrality and $\Delta\eta$ windows, is corrected for acceptance and detector inefficiencies. The results presented here are not corrected for global charge conservation.

Previously the STAR Collaboration [10] studied net-charge fluctuations in different center-of-mass energies from 19.6 to 200 GeV and in a symmetric range about mid-rapidity and with relative particle pseudorapiditiy <1.0. The results for gold-gold (AuAu) collisions at $\sqrt{s_{_{\mathrm{NN}}}} = 200\,\mathrm{GeV}$ with maximum relative particle pseudorapidity $\Delta\eta = 1.0$ are consistent with the HRG theoretical predictions. A similar measurement is reported by the ALICE Collaboration [11] in lead-lead (PbPb) collisions at $\sqrt{s_{_{\mathrm{NN}}}} = 2.76\,\mathrm{TeV}$ in terms of $\nu_{(+-,\mathrm{dyn})}$ in symmetric ranges about mid-rapidity with $\Delta\eta = 1.0$ and 1.6 ranges, consistent with the HRG and close to the QGP limits, respectively. The aforementioned fluctuations predicted for the QGP might be detectable in case they are measured over a very large rapidity range (of order of four units in $\Delta\eta$) [12, 13, 17]. The measurement presented in this note provides a broad rapidity coverage, which could further reveal initial-state fluctuations and particle production mechanisms. More specifically, we extend the extractions of $\nu_{(+-,\mathrm{dyn})}$ and D up to $\Delta\eta = 4.8$ using PbPb and pp collisions at $\sqrt{s_{_{\mathrm{NN}}}} = 5.02\,\mathrm{TeV}$, recorded in 2018 and 2017 by the CMS detector and corresponding to integrated luminosities of 0.607 and $252\,\mathrm{nb}^{-1}$ [18–23], respectively. We compare our results with the predictions from HYDJET (version 1.8) [24] and HIJING (version 1.3) [25] event generators in PbPb collisions in an extended centrality range, and with those from the PYTHIA8 (version 2.1.2) [26] event generator in pp collisions.

2 The CMS detector

The central feature of the CMS apparatus is a superconducting solenoid of 6 m internal diameter, providing a magnetic field of 3.8 T. Within the solenoid volume there is a silicon pixel and strip tracker, a lead tungstate crystal electromagnetic calorimeter (ECAL) and a brass and scintillator hadron calorimeter (HCAL), each composed of a barrel and two endcap sections. The silicon tracker consists of 1856 silicon pixel and 15,148 silicon strip detector modules. The silicon tracker measures charged particles within the range $|\eta| < 3.0$, and provides track resolutions of typically 1.5% in p_{T} and 20–75 μm in the transverse impact parameter [27, 28] in pixel detector for nonisolated particles of $1 < p_{\mathrm{T}} < 10$ GeV [29]. The forward hadron (HF) calorimeter uses steel as an absorber and quartz fibers as the sensitive material. The two halves of the HF are located 11.2 m (in z) from the interaction region, one on each end, and together they provide coverage in the range $3.0 < |\eta| < 5.2$. The HF calorimeters are subdivided into "towers" with $\Delta\eta \times \Delta\phi = 0.175 \times 0.175$. Energy deposited in a tower is treated as a detected hadron in this analysis. The HF calorimeters also serve as luminosity monitors. Muons are measured in gas-ionization detectors embedded in the steel flux-return yoke outside the solenoid. A more detailed description of the CMS detector, together with a definition of the coordinate system used and the relevant kinematic variables can be found in Ref. [30].

3 Data samples and event selections

The analysis presented in this note makes use of approximately 4 and 15 billion "minimum-bias" (MB) triggered events from PbPb and pp collisions, respectively. The MB events are selected online by requiring signals above the readout threshold of 3 GeV in each of the HF calorimeters [29, 31]. Background events due to beam-gas interactions and non-hadronic collisions are filtered out offline. The events used in this analysis are required to have at least one primary interaction vertex determined with two or more tracks [27] within a distance of 15 cm from the center of the nominal interaction point along with the beam axis and to have at least two calorimeter towers in each HF detector with energy deposits of more than 4 GeV per tower. In the case of PbPb collisions, the primary interaction vertex is considered as the reconstructed vertex with the highest number of associated tracks (described in Section 9.4.1 of Ref. [32]). When measuring the net-charge fluctuations in pp collisions instead, the same event may contain multiple independent interactions (pileup), hence primary interaction vertices. All tracks with $0.5 < p_{\mathrm{T}} < 3.0$ GeV and $|\eta| < 2.4$, and associated to a primary interaction vertex, must pass the high-purity selection criteria described in Ref. [5, 33]. The relative uncertainty in the p_{T} measurement must be less than 0.1. In PbPb collisions, additional selections are applied to the tracks: the number of hits in the silicon tracker should be larger than 11 and the normalized χ^2 per layer of the silicon detector must be less than 0.18. The collision centrality is defined as a fraction of the inelastic hadronic cross section, with 0% corresponding to the full overlap of the two colliding nuclei.

The experimental results presented in the study are compared with the predictions from Monte Carlo event generators. The HIJING generator is a combination of the initial nucleon-nucleon interactions and the subsequent parton dynamics, whereas HYDJET is an extension of HIJING that combines the initial-state parton production from HIJING with the final-state hydrodynamic evolution of the created medium. It includes both hard scatterings and soft interactions. The PYTHIA program includes models for hard scatterings, initial- and final-state radiation, hadronization processes, and final-state hadron decays. It incorporates a range of physics models and parameters to describe various aspects of the collision, such as parton fragmentation, particle production, and decay processes. The Monte Carlo simulations of the CMS detector response are performed using the GEANT4 [34] framework in the analysis.

4 Systematic uncertainty

We follow a similar procedure to estimate the systematic uncertainties in $\nu_{(+-,\mathrm{dyn})}$ values for both of PbPb and pp collisions. The systematic uncertainties related to the primary-vertex (z_{vtx}) reconstruction are obtained from the variations with different z_{vtx} locations from -15 to 15 cm. The selection criteria for the transverse and longitudinal track impact parameters, expressed as a function of their uncertainties, range from 2 to 5 standard deviations. In addition, the variation of relative uncertainty in p_{T} ranges from 5% to 10% and the normalized χ^2 per tracker layer in the range of 0.15–0.18 is also considered. The systematic uncertainty due to the different track selection requirement is found to be the leading one for this measurement. Moreover, the centrality calibration is varied as an additional source of systematic uncertainty in PbPb collisions. The uncertainties due to the comparison between simulated and reconstructed tracks are taken into account in this measurement. We also consider the systematic uncertainties due to the tracking efficiency by comparing values with and without applying the correction in data. Finally, in the case of pp collisions, the impact of pileup is also considered by varying the pileup selection by considering the distance among reconstructed vertices and their asso-

ciate number of tracks. In order to estimate uncertainties from different sources in each $\Delta\eta$ and centrality bin, the relative differences are fitted with a polynomial function. The relative systematic uncertainties from each source are evaluated from the difference between the nominal and varied results. The systematic uncertainty for the $\langle N_{\rm ch}\rangle\ \nu_{(+-,{\rm dyn})}$ value at $\Delta\eta$ = 4.8 ranges from 0.3% in the 70-80% centrality bin to 11% in the 0-5% centrality bin.

5 Results and discussion

5.1 Centrality dependence

Figure 1 (left panel) presents the measurement of $\nu_{(+-,{\rm dyn})}$ as a function of centrality for various $\Delta\eta$ windows: 1.0, 1.6 and 4.8. The $\nu_{(+-,{\rm dyn})}$ values are consistently negative, indicating that the contributions from the correlations of opposite-sign particles dominate as compared to same-sign particles [15]. The value of $\nu_{(+-,{\rm dyn})}$ is found to become more negative with increasing centrality or, correspondingly, decreasing particle multiplicity. In central collisions, where charged particle multiplicities are higher, the absolute value of $\nu_{(+-,{\rm dyn})}$ approaches monotonically to zero. The statistical and systematic uncertainties are smaller than the marker size, indicating the precision of the measurement. No correction has been applied for the effect of global-charge conservation. This correction is model dependent and beyond the scope of the current presentation.

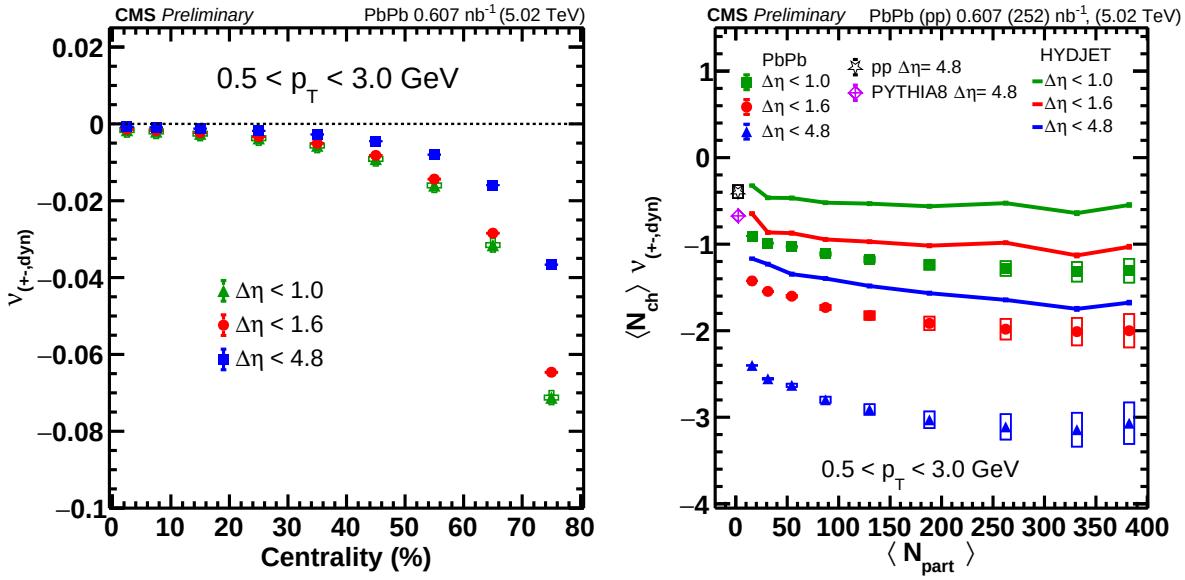

Figure 1: Summary of the measured (left panel) $\nu_{(+-,{\rm dyn})}$ as a function of centrality and (right panel) $\langle N_{\rm ch}\rangle\nu_{(+-,{\rm dyn})}$ as a function of the average number of participating nucleons ($\langle N_{\rm part}\rangle$) for PbPb and pp collisions at 5.02 TeV. The horizontal line corresponds to zero net-charge fluctuations. The rectangular open boxes represent the systematic uncertainty and the vertical bars indicate the statistical uncertainty. On the right panel, the predictions from HYDJET [24] and PYTHIA8 [26] event generators in PbPb and pp collisions, respectively, are also shown.

Figure 1 (right panel) shows the values of $\langle N_{\rm ch}\rangle\ \nu_{(+-,{\rm dyn})}$ as a function of the average number of participating nucleons ($\langle N_{\rm part}\rangle$) [35] in both the systems. This comparison helps to understand how the properties of the colliding system, such as its size and energy density, affect the net-charge fluctuation per entropy dependence. The values of $\langle N_{\rm ch}\rangle\ \nu_{(+-,{\rm dyn})}$ obtained using the larger $\Delta\eta$ window of 4.8 are compared to those obtained using the smaller windows of 1.0 and 1.6 for all centrality classes. The experimental findings demonstrate that the value $\langle N_{\rm ch}\rangle$

$\nu_{(+-,\mathrm{dyn})}$ values become significantly more negative with an increase in the $\Delta\eta$ range. The values based on the HYDJET and HIJING event generators show a similar trend with increasing multiplicity, although with reduced magnitude.

In addition to PbPb collisions, the measurement also includes results from pp collisions. It is observed that the scaled value of $\nu_{(+-,\mathrm{dyn})}$ in pp collisions is larger than the values found for PbPb collisions. The model prediction from PYTHIA has a similar value and is consistent with the prediction from the HRG limit. However, it is important to note that none of the models fully explain the experimental data. This indicates that there may be additional physics effects or mechanisms at play that are not captured by the current models.

5.2 Pseudorapidity dependence

We explore the value of $\langle N_{\mathrm{ch}} \rangle \nu_{(+-,\mathrm{dyn})}$ within an extended $\Delta\eta$ coverage. This is the first time a net-charge fluctuation measurement has been done that extends the pseudorapidity coverage to the range where significant influence of the QGP phase [17] is expected. A better understanding of how global charge conservation affects the results is needed to firmly establish the QGP influence. The $\langle N_{\mathrm{ch}} \rangle \nu_{(+-,\mathrm{dyn})}$ value decreases with an increasing $\Delta\eta$ window as a consequence of the increase in charged particle multiplicities. The diffusion of charged hadrons in the rapidity space leads to the fluctuations getting weaker as the system evolves from the hadronic to the kinetic freeze-out phase [11, 36, 37]. The fluctuations created in the initial state can survive until the hadronic freeze-out in case of a rapid expansion of the primordial medium. Therefore, the smaller $\Delta\eta$ windows might not be ideal to capture the majority of the initial fluctuations [38]. Figure 2 shows the dependence of $\langle N_{\mathrm{ch}} \rangle \nu_{(+-,\mathrm{dyn})}$ as a function of $\Delta\eta$ in different centrality bins. For the most central 0–5% and mid-central 15–20%, the value of $\langle N_{\mathrm{ch}} \rangle \nu_{(+-,\mathrm{dyn})}$ for maximum $\Delta\eta$ lies between -3.0 to -2.0. The predictions from HYDJET and HIJING show a similar decreasing trend with $\Delta\eta$.

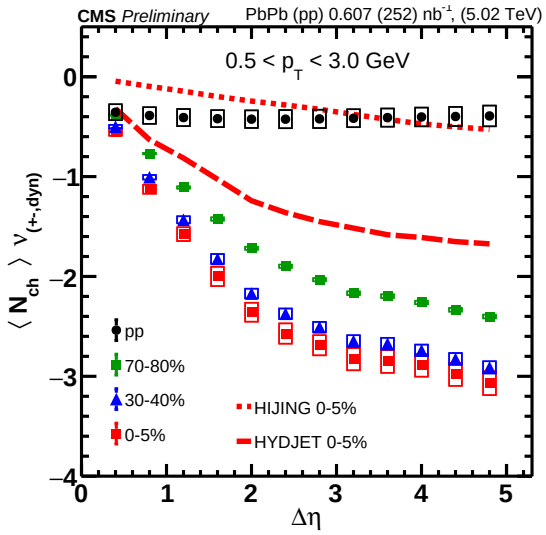

Figure 2: The measured $\langle N_{\mathrm{ch}} \rangle \nu_{(+-,\mathrm{dyn})}$ as a function of $\Delta\eta$ for different centrality ranges. The results are presented both in PbPb and pp collisions. The rectangular open boxes represent the systematic uncertainties, while the vertical bars indicate the statistical uncertainties. The dotted and dashed lines indicate the results from HIJING [25] and HYDJET [24] event generators, respectively.

The $\langle N_{\mathrm{ch}} \rangle \nu_{(+-,\mathrm{dyn})}$ value for the HIJING simulation in the 0–5% centrality class is close to 0 and consistent with the theoretical prediction of uncorrelated pion gas, while the HYDJET value is

within the HRG limit.

In Fig. 3, the $\langle N_{\rm ch}\rangle\nu_{(+-,dyn)}$ (plotted on the left y-axis) and the D (plotted on the right y-axis) values are presented for the 0–5% centrality class, along with theoretical predictions as a function of the pseudorapidity window. The predictions for a HRG are represented by the dotted line, while the predictions for the QGP formation are indicated by the band. The theoretical calculation of the $D-$ value does not account for the $\Delta\eta$ dependence. The net-charge fluctuations measured at $\Delta\eta < 1.0$ are found compatible with HRG expectations, as also reported by STAR [10] and ALICE [1]. Although the relative influence of the hadronic and QGP states will require a better understanding of the role of net-charge conservation on the results, the extent of the pseudorapidity window in Fig. 3 is such that a significant QGP influence is expected for the larger values of $\Delta\eta$.

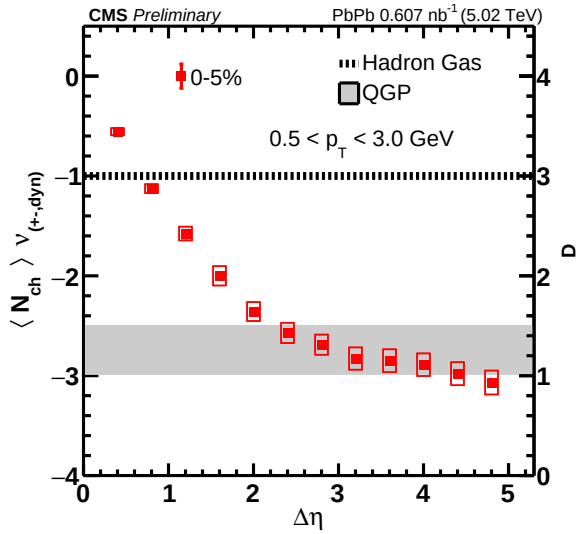

Figure 3: $\langle N_{\rm ch}\rangle\nu_{(+-,\rm dyn)}$ (left y-axis) and D-measure (right y-axis) values as a function of $\Delta\eta$ for the 0–5% centrality class. The rectangular open boxes represent the systematic uncertainties, while the vertical bars indicate the statistical uncertainties. The theoretical predictions for the HRG [12, 13, 16, 17] and QGP [12, 13, 16, 17] limits are indicated with the dotted line and band, respectively.

6 Summary

In this note, the dynamical net-charge fluctuations in terms of $\nu_{(+-,\rm dyn)}$ in lead-lead (PbPb) and proton-proton (pp) collisions at $\sqrt{s_{\rm NN}}$ = 5.02 TeV are reported. The measurement takes advantage of the large pseudorapidity coverage of the CMS detector to, for the first time, determine the dynamical net-charge fluctuations in pseudorapidity windows where the influence of the QGP state is expected to be significant. The $\nu_{(+-,\rm dyn)}$ values are found to become increasingly more negative going from central to peripheral collisions. The $\nu_{(+-,\rm dyn)}$ values are found to be negative in all cases, implying the dominance of the correlation of opposite sign charged particles. We also determine the charged particle multiplicity and $\Delta\eta$ window dependence of the product $\nu_{(+-,\rm dyn)}$, where this product is related to the charge particle fluctuations per entropy. We find the $\langle N_{\rm ch}\rangle$ $\nu_{(+-,\rm dyn)}$ values decrease monotonically with increasing relative pseudorapidity window ($\Delta\eta$) for all centrality ranges. Firm conclusions based on the current experimental results require a better understanding of how global charge conservation affects the fluctuation observables.

References

[1] STAR Collaboration, "Experimental and theoretical challenges in the search for the quark gluon plasma: The STAR Collaboration critical assessment of the evidence from RHIC collisions", *Nucl. Phys. A* **757** (2005) 102, doi:10.1016/j.nuclphysa.2005.03.085, arXiv:nucl-ex/0501009.

[2] PHENIX Collaboration, "Formation of dense partonic matter in relativistic nucleus-nucleus collisions at RHIC: experimental evaluation by the PHENIX Collaboration", *Nucl. Phys. A* **757** (2005) 184, doi:10.1016/j.nuclphysa.2005.03.086, arXiv:nucl-ex/0410003.

[3] BRAHMS Collaboration, "Quark-gluon plasma and color glass condensate at RHIC? The perspective from the BRAHMS experiment", *Nucl. Phys. A* **757** (2005) 1, doi:10.1016/j.nuclphysa.2005.02.130, arXiv:nucl-ex/0410020.

[4] PHOBOS Collaboration, "The PHOBOS perspective on discoveries at RHIC", *Nucl. Phys. A* **757** (2005) 28, doi:10.1016/j.nuclphysa.2005.03.084, arXiv:nucl-ex/0410022.

[5] CMS Collaboration, "Charged-particle nuclear modification factors in PbPb and pPb collisions at $\sqrt{s_{\mathrm{NN}}} = 2.76$ TeV", *JHEP* **04** (2017) 39, doi:10.1007/jhep04(2017)039, arXiv:1611.01664.

[6] PHOBOS Collaboration, "High transverse momentum triggered correlations over a large pseudorapidity acceptance in AuAu collisions at $\sqrt{s_{\mathrm{NN}}} = 200$ GeV", *Phys. Rev. Lett.* **104** (2010) 062301, doi:10.1103/PhysRevLett.104.062301, arXiv:0903.2811.

[7] CMS Collaboration, "Long-range and short-range dihadron angular correlations in central PbPb collisions at $\sqrt{s_{\mathrm{NN}}} = 2.76$ TeV", *JHEP* **07** (2011) 076, doi:10.1007/jhep07(2011)076, arXiv:1105.2438.

[8] CMS Collaboration, "Observation of long-range, near-side angular correlations in pPb collisions at the LHC", *Phys. Lett. B* **718** (2013) 795, doi:10.1016/j.physletb.2012.11.025, arXiv:1009.4122.

[9] CMS Collaboration, "Measurement of long-range near-side of long-range near-side two-particle angular correlations in pp collisions at $\sqrt{s} = 13$ TeV", *Phys. Rev. Lett.* **116** (2016) 172302, doi:10.1103/PhysRevLett.116.172302, arXiv:1510.03068.

[10] STAR Collaboration, "Beam-energy and system-size dependence of dynamical net-charge fluctuations", *Phys. Rev. C* **79** (2009) 024906, doi:10.1103/PhysRevC.79.024906, arXiv:0807.3269.

[11] ALICE Collaboration, "Net-charge fluctuations in PbPb collisions at $\sqrt{s_{\mathrm{NN}}} = 2.76$ TeV", *Phys. Rev. Lett.* **110** (2013) 152301, doi:10.1103/PhysRevLett.110.152301, arXiv:1207.6068.

[12] S. Jeon and V. Koch, "Charged particle ratio fluctuation as a signal for quark-gluon plasma", *Phys. Rev. Lett.* **85** (2000) 2076, doi:10.1103/PhysRevLett.85.2076, arXiv:hep-ph/0003168.

[13] M. Asakawa, U. W. Heinz, and B. Muller, "Fluctuation probes of quark deconfinement", *Phys. Rev. Lett.* **85** (2000) 2072, doi:10.1103/PhysRevLett.85.2072, arXiv:nucl-th/0106046.

[14] S. Ghosh, P. Mali, and A. Mukhopadhyay, "Net-charge fluctuation in AuAu collisions at energies available at the Facility for Antiproton and Ion Research using the UrQMD model", *Phys. Rev. C* **96** (2017) 024912, doi:10.1103/PhysRevC.96.024912, arXiv:1805.00790.

[15] M. Bleicher, S. Jeon, and V. Koch, "Event-by-event fluctuations of the charged particle ratio from nonequilibrium transport theory", *Phys. Rev. C* **62** (2000) 061902, doi:10.1103/PhysRevC.62.061902, arXiv:hep-ph/0006201.

[16] S. Jeon and V. Koch, "Fluctuations of particle ratios and the abundance of hadronic resonances", *Phys. Rev. Lett.* **83** (1999) 5435, doi:10.1103/PhysRevLett.83.5435, arXiv:nucl-th/9906074.

[17] S. Jeon and V. Koch, "Event by event fluctuations", p. 430. 2004. arXiv:hep-ph/0304012. doi:10.1142/9789812795533_0007.

[18] CMS Collaboration, "Precision luminosity measurement in proton-proton collisions at $\sqrt{s} = 13$ TeV in 2015 and 2016 at CMS", *Eur. Phys. J. C* **81** (2021) 800, doi:10.1140/epjc/s10052-021-09538-2, arXiv:2104.01927.

[19] CMS Collaboration, "CMS luminosity measurement using nucleus-nucleus collisions at $\sqrt{s_{\mathrm{NN}}} = 5.02$ TeV in 2018", CMS Physics Analysis Summary CMS-PAS-LUM-18-001, 2022.

[20] CMS Collaboration, "CMS luminosity measurement for the 2017 data-taking period at $\sqrt{s}$ = 13 TeV", CMS Physics Analysis Summary CMS-PAS-LUM-17-004, 2018.

[21] CMS Collaboration, "CMS luminosity measurement for the 2018 data-taking period at $\sqrt{s}$ = 13 TeV", CMS Physics Analysis Summary CMS-PAS-LUM-18-002, 2019.

[22] CMS Collaboration, "Jet performance in pp collisions at $\sqrt{s} = 7$ TeV", CMS Physics Analysis Summary CMS-PAS-JME-10-003, 2010.

[23] CMS Collaboration, "Tracking POG results for pion efficiency with the D^* meson using data from 2016 and 2017", CMS Detector Performance Note CMS-DP-2018-050, 2018.

[24] I. Lokhtin et al., "Heavy ion event generator HYDJET++ (hydrodynamics plus jets)", *Comput. Phys. Comm.* **180** (2009) 779, doi:10.1016/j.cpc.2008.11.015, arXiv:0809.2708.

[25] Z. Moravcova, K. Gulbrandsen, and Y. Zhou, "Generic algorithm for multiparticle cumulants of azimuthal correlations in high-energy nucleus collisions", *Phys. Rev. C* **103** (2021) 024913, doi:10.1103/PhysRevC.103.024913, arXiv:2005.07974.

[26] P. Skands, S. Carrazza, and J. Rojo, "Tuning PYTHIA 8.1: the Monash 2013 tune", *Eur. Phys. J. C* **74** (2014) 3024, doi:10.1140/epjc/s10052-014-3024-y, arXiv:1404.5630.

[27] CMS Collaboration, "Description and performance of track and primary-vertex reconstruction with the CMS tracker", *Journal of Instrumentation* **9** (2014) P10009, doi:10.1088/1748-0221/9/10/p10009, arXiv:1405.6569.

[28] CMS Collaboration, "Track impact parameter resolution for the full pseudorapidity coverage in the 2017 dataset with the CMS Phase-1 Pixel detector", CMS Detector Performance Summary CMS-DP-2020-049, 2020.

[29] Tracker Group of the CMS Collaboration, "The CMS phase-1 pixel detector upgrade", *JINST* **16** (2021) P02027, doi:10.1088/1748-0221/16/02/P02027, arXiv:2012.14304.

[30] CMS Collaboration, "The CMS experiment at the CERN LHC", *JINST* **3** (2008) S08004, doi:10.1088/1748-0221/3/08/S08004.

[31] CMS Collaboration, "The CMS trigger system", *JINST* **12** (2017) P01020, doi:10.1088/1748-0221/12/01/P01020, arXiv:1609.02366.

[32] CMS Collaboration, "Technical proposal for the Phase-II upgrade of the Compact Muon Solenoid", CMS Technical Proposal CERN-LHCC-2015-010, CMS-TDR-15-02, 2015.

[33] CMS Collaboration, "Observation and studies of jet quenching in PbPb collisions at nucleon-nucleon center-of-mass energy = 2.76 TeV", *Phys. Rev. C* **84** (2011) doi:10.1103/PhysRevC.84.024906, arXiv:1102.1957.

[34] GEANT4 Collaboration, "GEANT4 — a simulation toolkit", *Nucl. Instrum. Meth. A* **506** (2003) 250, doi:10.1016/S0168-9002(03)01368-8.

[35] CMS Collaboration, "Observation of the B_c^+ meson in PbPb and pp collisions at $\sqrt{s_{NN}} = 2.76$ TeV and measurement of its nuclear modification factor", *Phys. Rev. Lett.* **128** (2022) 252301, doi:10.1103/PhysRevLett.128.252301, arXiv:2201.02659.

[36] C. Pruneau et al., "Unified balance functions", 2022. arXiv:2209.10420.

[37] M. A. Stephanov, K. Rajagopal, and E. V. Shuryak, "Signatures of the tricritical point in QCD", *Phys. Rev. Lett.* **81** (1998) 4816, doi:10.1103/PhysRevLett.81.4816, arXiv:hep-ph/9806219.

[38] V. Koch, "Fluctuations and correlations in heavy ion collisions", *J . Phys.: Conf. Ser.* **50** (2006) 95, doi:10.1088/1742-6596/50/1/011.